JOURNAL OF RHEOLOGY

Extensional flow-induced crystallization of isotactic poly-1-butene using a filament stretching rheometer

Manojkumar Chellamuthu, Deepak Arora, H. Henning Winter, and Jonathan P. Rothstein

Citation: J. Rheol. **55**, 901 (2011); doi: 10.1122/1.3593471
View online: http://dx.doi.org/10.1122/1.3593471
View Table of Contents: http://www.journalofrheology.org/resource/1/JORHD2/v55/i4
Published by the The Society of Rheology

Extensional flow-induced crystallization of isotactic poly-1-butene using a filament stretching rheometer

Manojkumar Chellamuthu

Department of Mechanical and Industrial Engineering, University of Massachusetts, Amherst, Massachusetts 01003

Deepak Arora and H. Henning Winter

Department of Chemical Engineering, University of Massachusetts, Amherst, Massachusetts 01003

Jonathan P. Rothstein[a)]

Department of Mechanical and Industrial Engineering, University of Massachusetts, Amherst, Massachusetts 01003

(Received 4 August 2010; final revision received 20 April 2011; published 27 May 2011)

Synopsis

A filament stretching rheometer is used to investigate the extensional flow-induced crystallization of two commercial grade isotactic poly-1-butene samples. The degree of crystallinity of the stretched fibers is quantified using differential scanning calorimetry measurements as a function of extension rate and accumulated Hencky strains. All the measurements are performed using the Janeschitz-Kriegel protocol. The samples are first melted to erase their thermal and mechanical history. They are then quickly quenched to $T=98\,^{\circ}\mathrm{C}$ after which the stretch is imposed. The deformed filament is then allowed to crystallize fully at $T=98\,^{\circ}\mathrm{C}$. The extensional rheology of both the samples shows only minimal strain hardening. For the case of the lower molecular weight sample, the percent crystallinity increases from 46% under quiescent conditions to a maximum of 63% at an extension rate of $\dot{\varepsilon}=0.05\ \mathrm{s}^{-1}$. This corresponds to an increase of nearly 50% above the quiescent case. The high molecular weight sample shows similar trends achieving an increase in crystallinity of 25%. The experiments show an optimal extension rate for which the extensional flow has the maximum impact on the polymer crystallinity. The percent crystallinity of both the samples is observed to increase with increasing strain for a fixed extension rate. Small angle X-ray scattering shows that the observed increase in crystallinity is likely due to the increasing orientation and alignment of the polymer chains in extensional flows which enhances the thread-like precursors responsible for the formation of the crystals in the shish-kebab morphology. © *2011 The Society of Rheology.* [DOI: 10.1122/1.3593471]

I. INTRODUCTION

It is generally accepted in polymer processing that the crystallization of polymer melts can be significantly enhanced by the application of flow. The application of a flow during

[a)]Electronic mail: rothstein@ecs.umass.edu

or after crystallization of the polymer melt can produce molecular orientation which can dramatically affect the crystallization process. In some cases, flow-induced crystallization (FIC) can reduce the induction time for crystallization by an order of magnitude when compared to quiescent state [Haas and Maxwell (1969)]. Additionally, the oriented morphology resulting from FIC can enhance the mechanical properties of the final product by several orders of magnitude [McHugh (1995)]. Elongational flows are very important in many polymer processing techniques including fiber spinning, film blowing, and blow molding. In this paper, we will focus on the extensional flow-induced crystallization. A filament stretching rheometer will be used to impose a transient homogenous extensional flow of various strengths and durations on a series of isotactic poly-1-butene samples with a range of molecular weights.

Early works of FIC focused mainly on polymer solutions in stirred vessels [Pennings and Kiel (1965)]. Their results showed that unlike polymers crystallized under quiescent conditions which tend to form spherulites, polymers crystallized under flow can form a row-nucleated structures colloquially called "shish-kebabs." Shish-kebabs consists of a central fiber core surrounded by lamellar crystalline structures, periodically attached along the cylindrical core [Pennings and Kiel (1965)]. Keller and Kolnaar (1997) and Eder and Janeschitz-Kriegel (1997) showed that shear and extensional flows can facilitate nucleation through the formation of bundles of highly oriented chains. A great deal of research has been dedicated to shear-induced crystallization of polymer melts [Acierno *et al.* (2003); Eder and Janeschitz-Kriegel (1997); Elmoumni and Winter (2006); Elmoumni *et al.* (2003); Janeschitz-Kriegl (2003); Janeschitz-Kriegl *et al.* (2005); Janeschitz-Kriegl *et al.* (2003); Kumaraswamy *et al.* (2002); Pogodina *et al.* (1999); Seki *et al.* (2002); Winter *et al.* (2001)]. Take, for example, the work of Seki *et al.* (2002). They tested the role of long chains in enhancing the shear-induced crystallization kinetics and crystalline morphology using the blends with fractionated high molecular weight isotactic polypropylene (PP) and narrow molecular weight distribution blended with low molecular weight with PP base. According to their results, long chains play an important role in enhancing the formation of the thread-like precursors needed for the formation of shish-kebabs. They demonstrated that the chains with weight-average molecular weight five times higher than molecular weight of the base resin strongly affects the crystallization kinetics and morphology using *in situ* rheo-optical measurements and *ex situ* macroscopic observations. Kumaraswamy *et al.* [Kumaraswamy *et al.* (2002)] through their rheo-optical studies combined with synchrotron wide-angle X-ray diffraction showed evidence of highly oriented crystalline precursors by strongly shearing an isotactic polydisperse PP melt. Hadinata *et al.* (2007) used an up-shoot in shear viscosity to define a crystallization onset time to compare the shear-induced crystallization behavior of poly-1-butene samples with different molecular weight distribution. Their experimental investigations showed shorter onset times for higher molecular weight sample. According to their results, the transition from plateau to slope region occurs much earlier compared to lower molecular weight samples, which agrees with the fact the longer polymer chains crystallize faster under the influence of flow.

Several researchers have proposed that the dimensionless Weissenberg number, $Wi=\lambda\dot{\gamma}$, can be used as an important criterion to classify the strength of FIC [Acierno *et al.* (2003); Elmoumni *et al.* (2003); Somani *et al.* (2005); van Meerveld *et al.* (2004)]. Here λ is the characteristic relaxation time of the fluid and $\dot{\gamma}$ is the shear rate. Elmoumni *et al.* (2003) used the Weissenberg number to identify the shear-induced transition from isotropic (spherulite) to anisotropic (shish-kebabs) crystal growth. They concluded that at low Weissenberg numbers, $Wi<1$, the isotropic (spherulite) crystal growth still prevails due to relaxation of the flow-induced molecular deformation. However, even at these low

Weissenberg numbers, they found that the shear flow can increase the nucleation density. At higher strain rates and Weissenberg numbers, $Wi > 1$, the polymer chains are oriented and deformed by the flow resulting in anisotropic crystal growth in the form of shish-kebabs and a dramatic increase in the nucleation density.

Only a limited number of researchers have studied the effect of accumulated strain on shear-induced crystallization [Chai *et al.* (2003); Elmoumni and Winter (2006); Li and de Jeu (2003); Vleeshouwers and Meijer (1996)]. Vleeshouwers and Meijer (1996) demonstrated that longer pre-shearing of the isotactic polypropylenes (iPP) at the supercooled temperature gave shorter crystallization times. According to their results, accumulated strains of up to $\gamma = 1000$ kept reducing the crystallization times. Li and de Jeu (2003) used small-angle X-ray scattering and wide-angle X-ray diffraction simultaneously to show the formation of oriented precursors for crystallization by pre-shearing the iPP melt at a smaller strain of $\gamma = 15$. They did not report any results for large strain requirements for obtaining the oriented precursors for crystallization. Elmoumni and Winter (2006) demonstrated using polarized microscopy and light transmittance measurements that the strain requirement for iPP crystallization transition from spherulite to shish-kebab occurs at Weissenberg numbers of $Wi = 1$ and total strains of $\gamma = 600$. According to their results, total strains less than $\gamma < 600$ leads to spherulitic crystal morphology, whereas total strains greater than or equal to $\gamma \geq 600$ produce oriented crystal morphology.

Experimental studies on extensional flow-induced crystallization are more limited in number than those of shear-induced crystallization. In their pioneering experiments on the crystallization of polyethylene from xylene solutions under complex flow conditions, Pennings *et al.* (1970) showed the formation of shish-kebabs, which they attributed to the effective orientation of molecules in the regions of the stirring vessel and Couette cell where elongational flow components were present. According to Hoffman and Laurritzen (1961), the molecular orientation produced by the extensional flow leads to an effective change of the free energy of the polymer melt. This in turn directly increases the rate of nucleation by increasing the melting temperature of the resulting crystals and therefore the effective amount of supercooling of the polymer melt. Janeschitz-Kriegl *et al.* (2003) demonstrated through their experimental studies that extensional flow can enhance the rate of nucleation. Until very recently, most of the experiments on crystallization in extensional flows were carried out in polymer processing conditions, such as melt spinning [Chu and Hsiao (2001); Samon *et al.* (1999); Samon *et al.* (2000)], which involve complicated histories of shear and extension. Hence, there is still a clear need for experiments with a well-defined extensional flow, a constant extension rate and a well-controlled temperature protocol.

In more recent experiments, better-defined extensional flows have been imposed prior to crystallization. Swartjes *et al.* (2003) used a cross slot flow cell device to perform a comprehensive analysis on stress-induced crystallization in an extensional flow based on birefringence and wide-angle x-ray scattering (WAXS). Their birefringence and WAXS measurements showed the formation of highly oriented fiber-like crystal structure, which lasted for 20 min after the cessation of flow. Unfortunately, in their experiments the extension rate imposed on the polymer was not uniform and shear gradients exists close to observation windows, making it difficult to deconvolute the effect of shear from the effect of extension. Stadlbauer *et al.* (2004a, 2004b) developed an elongational rheometer to investigate the influence of creeping flow under a constant applied tensile stress on the structure development of two different linear iPP homopolymers. They showed a significant increase in the number density of nuclei with increasing mechanical work. Quite remarkably, they found that when the number density was compared against mechanical work rather than rate or strain independently, the data for both shear and extensional

flow-induced crystallization collapsed onto a single master curve. More recently, Hadinata *et al.* (2007) investigated the effect of elongational flow-induced crystallization of a high molecular weight isotactic poly-1-butene compared to shear-induced crystallization using a Sentmanat extensional rheometry (SER) fixture from a standard shear rheometer. They defined a crystallization onset time as the time at which an increase in extensional viscosity was observed. The crystallization onset time for elongational flow-induced crystallization was found to occur at 100th of the time needed under shear. These measurements demonstrate that extensional flow is much more effective at enhancing crystallization of polymer melts compared to simple shear flow. Unfortunately, due to the sagging of the samples after the flow-induced measurements, they were not able to stop the experiment to take samples for DSC or SAXS measurements that could be used to quantify the degree of crystallization. This limitation was very recently overcome by Sentmanat *et al.* (2010) who quickly quenched their SER stretched samples by opening the oven door immediately following the stretch and spraying the fluid filament with water. Subsequent differential scanning calorimetry (DSC) measurements on the ethylene-based butane plastomer melts following stretching within a SER at various temperatures, extension rates, and strains showed qualitative differences in the heat flow signatures. These differences included the appearance of a second peak in the DSC heat flow profile for stretched performed very close to the melt temperature and a clear increase in percent crystallinity when compared to the unstretched sample. Unfortunately, only the DSC profiles are presented and detailed trends in percent crystallinity and melt temperature with stretch rate, strain, and temperature are not included. In addition, the study does not present any microscopy or SAXS so the evolution of crystal size and structure with extension rate cannot be inferred from their data [Sentmanat *et al.* (2010)].

A major challenge to extensional flow-induced crystallization measurements is the imposition of a homogeneous extensional flow combined with a well-defined temperature protocol. Numerous devices including spin line rheometers, opposed jet device, and capillary rheometer have been used in past to study the extensional behavior of polymer melts [McKinley and Sridhar (2002)]. Unfortunately, each of these devices is plagued by an unknown prestrain history and some degree of shearing in the flow field. It is therefore very difficult to deconvolute the effect of shear from those of extension or clearly understand the importance of extension rate or accumulated strain on the crystallization dynamics. In this study, a filament stretching rheometer (FiSER) with a custom-built oven is used to investigate the extensional flow-induced crystallization of isotactic poly-1-butene melts. The FiSER is capable of imposing homogeneous uniaxial extensional flow with a constant extension rate while precisely controlling the temperature without the need to quench the sample following stretch. The main advantage of FiSER is that we can probe the effects of extensional flow and accumulated strain in enhancing the crystallization dynamics in the absence of shear.

The outline of the paper is as follows. In Sec. II, we briefly describe the implementation of filament stretching extensional rheometer with custom-built oven and test poly-1-butene melts used. In Sec. III A, we compare and discuss the extensional rheology of the polymer melts measured using filament stretching rheometer with shear rheology measurements. In Sec. III B, we quantify the degree of crystallinity of the stretched polymers obtained from differential scanning calorimetry and small-angle X-ray scattering measurements to help interpret the role of homogeneous extensional flows in crystallization dynamics. Finally, in Sec. IV we conclude.

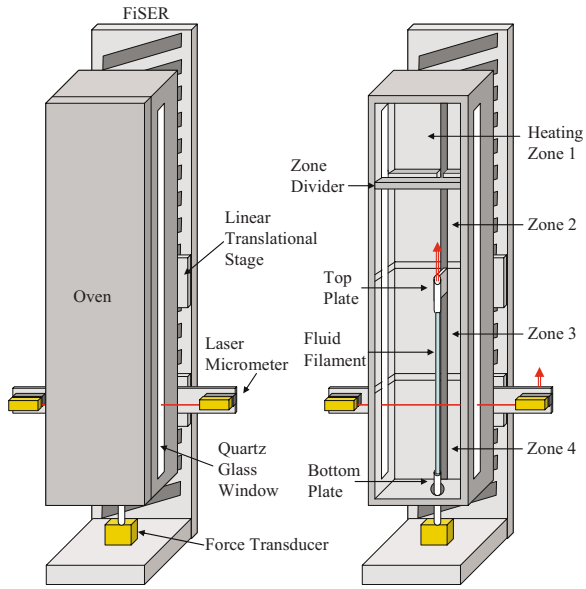

FIG. 1. A schematic diagram of a filament stretching rheometer with custom-built oven.

II. EXPERIMENTAL SETUP

A. Materials

Extensional flow-induced crystallization measurements are performed on DP0401M and PB0200 which are commercial grade poly-1-butene melts. The DP0401M has a weight-average molecular weight of $M_w = 176\,000$ g/mol and a polydispersity of 5.7. According to the GPC measurements from Basell, it has an isotacticity of 98.8% and it contains no nucleating agents. The PB0200 has a molecular weight of $M_w = 440\,000$ g/mol and a polydispersity of 11.6. All the samples are provided by Basell in the form of pellets. Among several crystal morphologies, only form II and form I are known to exist in poly-1-butene melt crystalline samples under quiescent conditions [Alfonso *et al.* (2001)]. All the crystallized samples exist as kinetically favorable form II crystals, which are characterized by a tetragonal unit cell. The transformation from form II to form I (stable hexagonal unit cell) crystals takes about ten days of aging at room temperature [Hadinata *et al.* (2007)]. The form I crystals exhibit melting point in the range of $118\,^{\circ}\mathrm{C} < T_{m\mathrm{I}} < 137\,^{\circ}\mathrm{C}$, which is higher than the melting point of the form II crystals that is typically between $108\,^{\circ}\mathrm{C} < T_{m\mathrm{II}} < 127\,^{\circ}\mathrm{C}$ $T_{m\mathrm{II}}$ [Alfonso *et al.* (2001); Azzurri *et al.* (2003)].

B. Filament stretching rheometry and experimental methods

An oven was designed, fabricated, and integrated into the filament stretching extensional rheometer. A representative sketch of a custom-built oven along with the filament stretching rheometer is shown in Fig. 1. The oven encloses the fluid filament as it stretches and can reach temperatures in excess of 300 °C. The oven has four separate zones divided by horizontal plates to reduce natural convection. All four zones are shown, however, for clarity only a single divider is shown in Fig. 1. Each zone is equipped with independent PID temperature control capable of maintaining the desired temperature with an accuracy of $\pm 1\,^{\circ}\mathrm{C}$.

A FiSER capable of imposing a homogeneous uniaxial extension on a fluid filament placed between its two endplates. A complete description of the design and operating space of the filament stretching rheometer used in these experiments can be found in McKinley and Sridhar (2002); Tirtaatmadja and Sridhar (1993) and a more detailed history of the technique can be found in the following papers by the McKinley and Sridhar groups [Anna and McKinley (2001); McKinley and Sridhar (2002); Tirtaatmadja and Sridhar (1993)]. In the filament stretching rheometer, an initially cylindrical filament of fluid is stretched between two circular endplates. The goal of the drive control system is to impose a motion on the endplates, $L(t)$, such that the resulting extension rate experienced by the fluid filament $\dot{\varepsilon}=-2/R_{\mathrm{mid}}(t)\ dR_{\mathrm{mid}}(t)/dt$, is held constant. Here $R_{\mathrm{mid}}(t)$ is the midplane radius. The strength of the extensional flow is described by the Weissenberg number, $Wi=\lambda\dot{\varepsilon}$. The total deformation of the fluid element is characterized by the Hencky strain, $\varepsilon=-2\ \ln(R_{\mathrm{mid}}/R_0)$. The midpoint diameter is measured with a laser micrometer mounted on the lower platen programed to follow the evolution of the midpoint of the elongating fluid filament. The elastic tensile stress difference generated within the filament, $\langle\tau_{zz}-\tau_{rr}\rangle$, is calculated from the force measured by the load cell taking into account the weight of the fluid, its surface tension and inertial effects [Anna *et al.* (2001)]. The extensional viscosity is then extracted from the principal elastic tensile stress by dividing by the extension rate, $\eta_E=\langle\tau_{zz}-\tau_{rr}\rangle/\dot{\varepsilon}$, and is often nondimensionalized by the zero shear rate viscosity to form the Trouton ratio, $Tr=\eta_E/\eta_0$. For a Newtonian fluid, $Tr=3$, while a non-Newtonian fluid can strain harden such that very large Trouton ratios can be achieved for Weissenberg numbers greater than $Wi>\frac{1}{2}$ [McKinley and Sridhar (2002)].

The Janeschitz-Kriegel protocol is used to study the extensional flow-induced crystallization of the polymer melts. In the Janeschitz-Kriegel protocol [Janeschitz-Kriegl and Eder (1990); Liedauer *et al.* (1993)], the sample is initially melted to erase its thermal history. The sample is then quickly quenched to an experimental temperature for crystallization, T_c, such that $T_c<T_m$. Once the sample has equilibrated at the crystallization temperature, a well-defined extensional flow is applied for a time chosen to be much shorter than crystal growth time. The goal is to only affect the nucleation process and not to disturb the crystal structure with flow. This requires careful choice of both the crystallization temperature and the flow rates.

The magnitude of extension rate prior to crystallization on the polymer melts was varied using our filament stretching rheometer to produce stretches with extension rates between $0.01\ \mathrm{s}^{-1}<\dot{\varepsilon}<10\ \mathrm{s}^{-1}$. Additionally, the total strain applied to the fluid filament was varied between $1<\varepsilon<5$. In this study, all the reported results were performed at a crystallization temperature of $T_c=98\,^{\circ}\mathrm{C}$. The fluid was initially melted at a temperature of $T=177\,^{\circ}\mathrm{C}$ and held there for 20 min to erase all the thermal and mechanical history. It was then quenched to $T_c=98\,^{\circ}\mathrm{C}$ at a rate of $10\,^{\circ}\mathrm{C/min}$. Once the fluid reached the crystallization temperature, it was held at that temperature for another minute to ensure a uniform temperature profile across the fluid filament before the stretch was imposed. All the stretched samples were allowed to crystallize post-stretch for 25 min at the crystallization temperature before a sample was cut from axial midpoint of the stretched filament for further testing.

The degree of crystallinity was tested using DSC (TA model DSC 1). The DSC was calibrated with high purity indium and benzoic acid and operating under purge nitrogen. The DSC was then used to characterize the crystallization behavior of all the stretched fibers. All the DSC traces were recorded from $25\,^{\circ}\mathrm{C}$ to $180\,^{\circ}\mathrm{C}$ at a heating rate of

10 °C/min. However, prior to the DSC measurements, the crystallized samples were stored at room temperature for 10 days to allow them to transform from form II crystals in to stable form I crystals.

Optical microscopy (Nikon TE2000-U) was performed through crossed polarizers to investigate the size and alignment of the polymer crystals in the fully crystallized samples. In addition, small-angle X-ray scattering (SAXS) measurements were performed to investigate the underlying structure and morphology of the polymer crystals formed in the filaments following stretch. SAXS measurements were performed at National Synchrotron Light Source, beamline X27C, at Brookehaven National Laboratory. The set up employed a 0.39 mm diameter X-ray beam with a wavelength of $\lambda = 0.1371$ nm. The sample to detector distance was calibrated using silver behenate standard peak at wave vector of $q = 1.076\ \text{nm}^{-1}$, where $q = (4\pi/\lambda)\sin\theta$ and 2θ is the scattering angle. The samples were cut from the axial midplane of the stretched filament and were mounted such that the extensional flow direction was aligned perpendicular to the beam direction so that any alignment of the crystals in the flow direction could be observed in the two-dimensional scattering patterns.

III. RESULTS AND DISCUSSIONS

A. Shear rheometry

The linear viscoelasticity of the polymer melts were characterized using a commercial rotational rheometer (Stresstech, ATS Rheosystems) using a 25 mm parallel plate geometry. The polymer pellets obtained from Basell were molded into flat 25 mm diameter disks using a hot press so they could be easily mounted within the rheometer. The disks were then placed on the shear rheometer, melted and then compressed to establish a uniform contact between the sample and rheometer plates. In Fig. 2, the linear viscoelastic response of both the DP0401M and PB0200 samples is shown. Time-temperature superposition is used to collapse the data from number of different temperatures into a single master curve for each molecular weight at a reference temperature equal to the crystallization temperature, $T_{ref} = T_c = 98\,^{\circ}\text{C}$. The storage, G', and loss modulus, G'', for both the samples are typical of a polydisperse linear melt. The cross-over point of the G' and G'' is indicative of the fluids relaxation time, λ. It is clear from Fig. 2 that PB0200 has a larger relaxation time and higher zero shear rate viscosity than the DP0401M which has a lower molecular weight. Note that it is the reptation or disengagement time, λ_d, that is of primary importance in extensional flows of polymer melts and will be used to evaluate the Weissenberg number, $Wi = \lambda_d \dot{\varepsilon}$, of these experiments because it is at $Wi > 0.5$ that the tube of constraints becomes aligned by the extensional flow [McKinley and Sridhar (2002); Rothstein and McKinley (2002)]. To determine the disentanglement time listed in Table I, IRIS was used to fit the data with a multimode Maxwell model. These fits are superimposed over the data in Fig. 2. The relaxation time was taken to be the viscosity-weighted-average relaxation time of the n-mode fit, $\lambda_d = \Sigma_{i=1}^{n} \eta_i \lambda_i / \Sigma_{i=1}^{n} \eta_i$. For entangled polymer melts, there are a number of other important relaxation times to consider including the Rouse time for the entire chain, $\lambda_R = \lambda_d M_e / 3M_w$, which for even a moderately entangled fluid is much smaller than the disentanglement time. The Rouse relaxation time can be related to the disengagement time by the average number of entanglements per chain, $Z = M_w / M_e$, such that $3Z\lambda_R = \lambda_d$ where $M_e = 14\,500$ g/mol is the entanglement molecular weight calculated from the shear rheology. As a result, for Weissenberg numbers larger than $Wi > 3M_w / M_e$, not only is the tube of constraints aligned

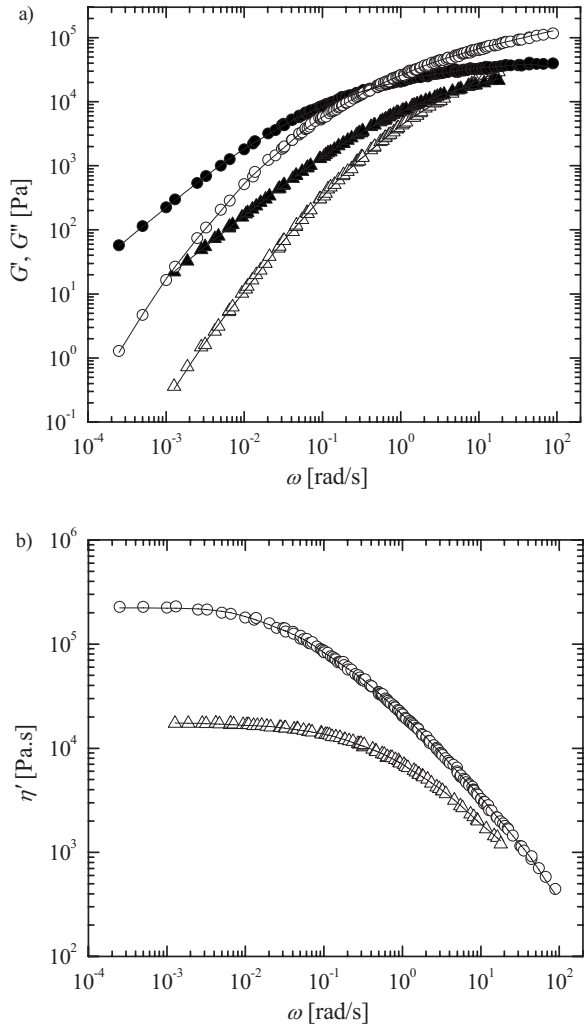

FIG. 2. The oscillatory shear master curves of DP0401M (△) and PB0200 (○) for a temperature of T_c=98 °C. Included in (a) are the solutions of modulus master curves with storage modulus G' (open symbols) and loss modulus G'' (filled symbols), while (b) includes complex viscosity master curves. Superimposed over both sets of data are solid lines representing the multimode Maxwell fits to each data set.

with the flow, but the polymer chains within the tube are also aligned and stretched. The value of disengagement time and the zero shear rate viscosity are reported in Table I at the reference temperature.

TABLE I. Zero-shear rate viscosity and relaxation times of poly-1-butene samples at T_c=98 °C.

Sample name	Zero-shear viscosity (Pa s)	λ_d (s)
DP0401M	1.7×10^4	19.4
PB0200	2.3×10^5	41.6

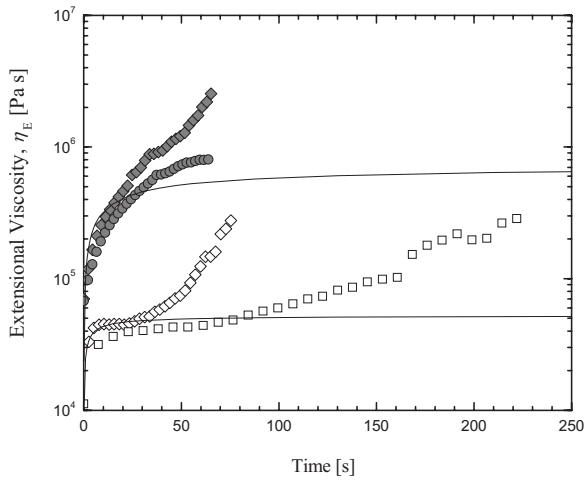

FIG. 3. FiSER measurements of the transient extensional viscosity as a function of time for different extension rates of poly-1-butene at $T=98\,^{\circ}\mathrm{C}$. Included are the solutions of extension rates of $\dot{\varepsilon}=0.01\ \mathrm{s}^{-1}$ (□), $0.02\ \mathrm{s}^{-1}$ (●), and $0.03\ \mathrm{s}^{-1}$ (♦). The open symbols correspond to DP0401M and filled symbols correspond to PB0200. The linear viscoelastic response is superimposed over the data.

B. Filament Stretching Rheometry

A series of transient extensional rheology measurements were performed on both the DP0401M and the PB0200 samples. In Fig. 3, a representative plots of extensional viscosity as a function of accumulated Hencky strain is presented for a series of extension rates at $T_c=98\,^{\circ}\mathrm{C}$. As seen in Fig. 3, the extensional rheology of both the samples is insensitive to all the tested strain rates over the range imposed. Only minimal strain hardening is achieved for all the extension rates corresponding to Trouton ratio values of approximately $Tr=\eta_E/\eta_0\approx 10$. Note that all these stretches were performed below $Wi<3M_w/M_e$ where no significant strain hardening is expected [McKinley and Sridhar (2002)]. These results are consistent with predictions of constitutive models for linear entangled polymer melts [Bhattacharjee *et al.* (2002)] as well as the response reported by Hadinata *et al.* (2007), who investigated the extensional rheology of a high molecular weight, poly-1-butene, BR200, over a similar extension rates varying between $0.0001\ \mathrm{s}^{-1}<\dot{\varepsilon}<10\ \mathrm{s}^{-1}$. In the section that follows, we will show that even in the absence of significant extensional thickening, the orientation and alignment of the tube of constraints resulting from the extensional flow imposed by the filament stretching rheometer is sufficient to dramatically affect the crystallization dynamics of these polymers melts.

C. DSC and SAXS

A series of DSC measurements was performed on the samples of DP0401M and PB0200 stretched over a broad range of extension rates and accumulated Hencky strains. In Fig. 4, a number of representational DSC curves of the heat flow as a function of temperature are shown. The experiments were chosen to compare the results for DP0401M samples with extension rates ranging from $\dot{\varepsilon}=0.01\ \mathrm{s}^{-1}$ to $\dot{\varepsilon}=0.5\ \mathrm{s}^{-1}$ and a fixed Hencky strain of $\varepsilon=5$. Additionally, an unstretched sample that was subjected to same temperature protocol is also shown in Fig. 4. When compared to an unstretched sample, it is clear from Fig. 4 that heat flow significantly increases with the imposition of

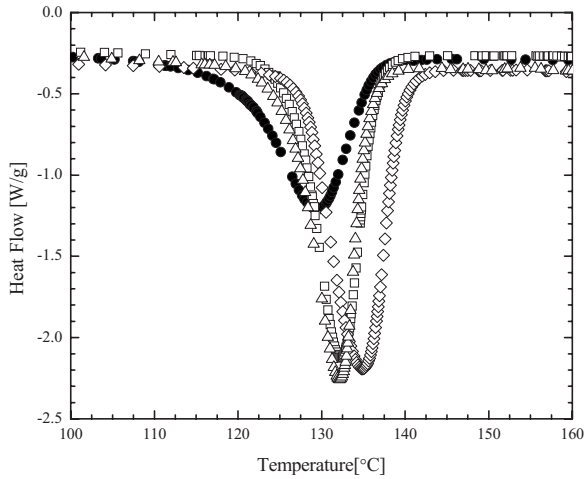

FIG. 4. A pictorial representation of DSC fits with heat flow as a function of temperature. Included are the solutions of PB 401M samples with extension rates $\dot{\varepsilon}=0.01\ s^{-1}$ (□), $0.04\ s^{-1}$ (◇), $0.5\ s^{-1}$ (△) all at a fixed strain of $\varepsilon=5$, and an unstretched sample (●).

an extensional flow prior to crystallization. For the quiescent case, the heat of fusion is 66 J/g, with the imposition of stretch, the heat of fusion increases from 77 to 89 J/g with increase in extension rate from $\dot{\varepsilon}=0.01\ s^{-1}$ to $\dot{\varepsilon}=0.04\ s^{-1}$. Additionally, the DSC curves demonstrate an increase in melting temperature and a sharpening of the DSC peak with an increasing extension rate to $\dot{\varepsilon}=0.04\ s^{-1}$. This trend is consistent with an increase in the number of nucleation sites, a move toward more uniform crystal size in the final solid and most importantly the presence of a highly aligned and oriented shish-kebab crystal structure [Keller and Kolnaar (1997)]. Beyond an extension rate of $\dot{\varepsilon}=0.04\ s^{-1}$, the heat of fusion and the peak melting temperature decrease slightly, but remain significantly higher than the quiescent state. These observations clearly demonstrate the ability of extensional flows to enhance the nucleation rate and crystallization kinetics of the poly-1-butene samples. The decrease in the heat flow for higher extension rates suggests that there is an optimal extension rate and strain for which extensional flow-induced crystallization produces maximum effect.

To analyze the DSC measurements more fully, the percent crystallinity is plotted in Fig. 5 as a function extension rate for DP0401M at a fixed strain of $\varepsilon=5$ and PB0200 at fixed strain of $\varepsilon=4$. Each data point in Fig. 5 represents an average of as few as three and as many as five individual measurements. The uncertainty in the degree of crystallinity data is typically $\pm 1\%$. It is clear from Fig. 5, that flow increases the degree of crystallinity when compared to the unstretched quiescent sample. However, the increase in crystallinity is not a monotonic function of extension rate for either sample. In each case, there is a critical extension rate above which a decrease in the crystallinity is observed with increasing extension rate. At very large extension rates, the degree of crystallinity appears to plateau at values of approximately 58% and 49% for the DP0401M and PB0200, respectively. For the case of DP0401M, the percent crystallinity increases from 46% to 63% with the increase in extension rate from the quiescent state to $\dot{\varepsilon}=0.05\ s^{-1}$. This represents an increase of nearly 50% above the quiescent case for the DP0401M. A similar increase of more than 25% is observed for PB0200 over the same change of extension rates.

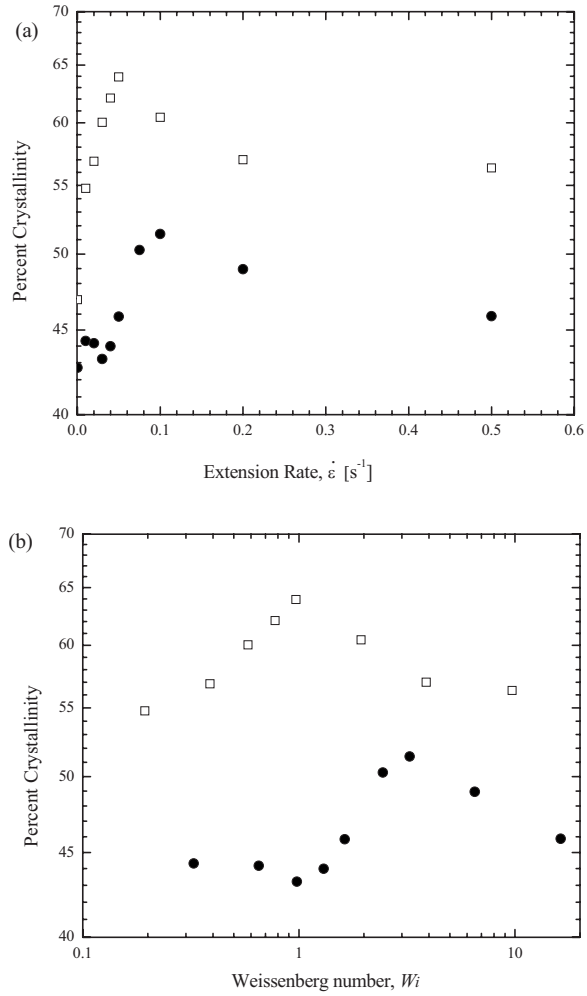

FIG. 5. Percent crystallinity as a function of (a) extension rate and (b) Weissenberg number for isotactic poly-1-butene samples at $T_c = 98\,^{\circ}\mathrm{C}$. Included are the solutions for DP0401M (□) at a fixed strain of $\varepsilon = 5.0$ and PB 0200 (●) at a fixed strain of $\varepsilon = 4.0$.

As shown in Fig. 5, the DSC trends for PB0200 are very similar when compared to DP0401M. Unlike DP0401M, which showed enhanced crystallization even at the lowest extension rates tested, the percent crystallinity of the PB0200 is insensitive to the changes in extension rate until the extension rate of $\dot{\varepsilon} = 0.04\ \mathrm{s}^{-1}$. At the lower extension rates, the flow is not fast enough to induce significant tube alignment as the tubes can relax back to their undeformed state more quickly than the flow can stretch them. This can be seen if the data are plotted against the extensional Weissenberg number as seen in Fig. 5(b). In Fig. 5(b), the onset of enhanced crystallization occurs around a Weissenberg number of $Wi \cong 1.0$ and the peak in the percent crystallinity for the PB0200 is observed to occur at a Weissenberg number of approximately $Wi \cong 3.0$. For the DP0401M, the onset and peak of enhanced crystallinity are found at a slightly lower Weissenberg numbers, $Wi \cong 0.4$ and $Wi \cong 1.0$, respectively. At around a Weissenberg number of one, the tube of constraints confining the entangled polymer melt align in the stretch direction which in turn promotes nucleation and growth of the polymer crystals [Elmoumni *et al.* (2003)]. It is, in

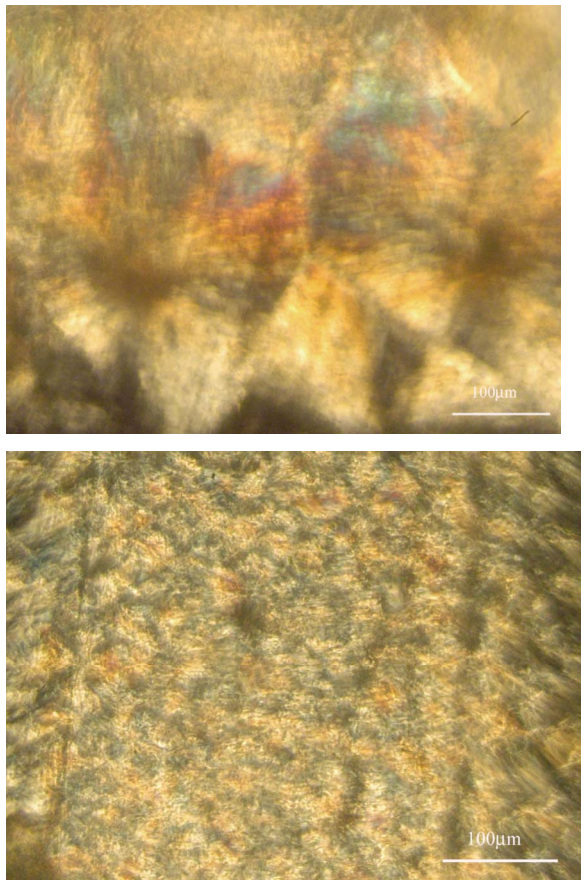

FIG. 6. Microscopy images taken through crossed polarizers of the DP0401M samples showing the size and alignment of crystals under (a) quiescent conditions ($\dot{\varepsilon}=0.0\ s^{-1}$) and (b) following a stretch with an extension rate of $\dot{\varepsilon}=0.05\ s^{-1}$ and an accumulated strain of $\varepsilon=5$. The stretch direction is aligned vertically.

fact, not until a much higher Weissenberg number, $Wi > 3M_w/M_e \cong 40$, that the polymer chains within the tube of constraints are stretched by the extensional flow. In our experiments, the Weissenberg number is always below this cutoff because the extension rates needed to reach this Weissenberg number are not possible in our extensional rheometer. These measurements demonstrate that the Weissenberg number is a suitable dimensionless criteria for quantifying the effect of extensional flow on enhanced crystallization in poly-1-butene melts. Similar conclusions have also been drawn from shear-induced crystallization experiments [Elmoumni *et al.* (2003)].

The increase in percent crystallinity with increasing extension rate or equivalently increasing Weissenberg number is likely due to the mechanism first proposed by Keller [Keller and Kolnaar (1997)], that is, the transition in crystalline morphology from a spherulite to a shish-kebab. Extensional flows tend to align polymer chains in the flow direction with the degree of orientation and polymer deformation increasing with extension rate. This polymer deformation, in turn, enhances the thread-like precursors which are responsible for the formation of the crystals in a shish-kebab morphology. If this hypothesis were true, then one would expect to see some evidence for the presence of shish-kebab structures in optical microscopy or SAXS or both. In Fig. 6, microscopy

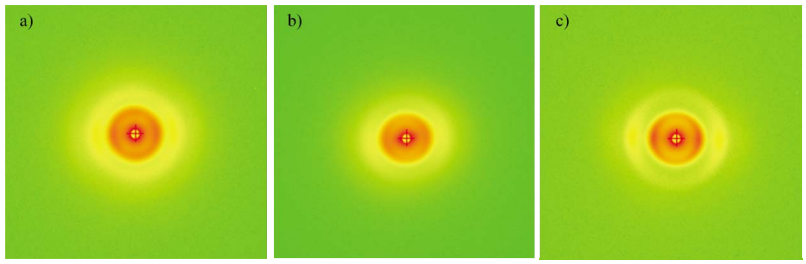

FIG. 7. Two dimensional small angle x-ray scattering patterns for DP0401M samples crystallized following stretches of extension rates of (a) $\dot{\varepsilon}=0.01\ s^{-1}$, (b) $\dot{\varepsilon}=0.05\ s^{-1}$, and (c) $\dot{\varepsilon}=0.5\ s^{-1}$. All stretches were performed to an accumulated strain of $\varepsilon=5$. The stretch direction is aligned horizontally to the scattering patterns.

images taken through crossed polarizers of two DP0401M samples are presented to illustrate the effect of extensional flow on the size, number, and alignment of the macroscopic polymer crystallites. In Fig. 6(a), an unstretched sample is shown. It can be concluded from the telltale Maltese cross patterns seen throughout the image that under quiescent conditions DP0401M forms large spherulites with diameters on the order of $d\sim 200\ \mu$m. In Fig. 6(b), a microscopy image taken through crossed polarizers of a sample stretched at an extension rate of $\dot{\varepsilon}=0.05\ s^{-1}$ is shown for comparison. This extension rate was chosen because it is near the point of maximum crystallinity measured through DSC (see Fig. 5). This microscopy image clearly shows that extensional flow both increases the number of nucleation sites and reduces, by approximately an order of magnitude, the size of the resulting spherulites. Further increasing the extension rate resulted in spherulites that were too small to see under optical microscopy and are therefore not included. In addition, there is a strong visual evidence to suggest that the imposed extensional flow has at least partially aligned the macroscopic crystal domains in the flow direction. This is likely the result of a transition with increasing extension rate from spherulite to shish-kebab morphology, a hypothesis that is corroborated by SAXS measurements.

SAXS was used to probe the crystalline morphology, alignment, and lattice spacing. In Fig. 7, the two-dimensional scattering patterns are shown for DP0401M crystallized under at three different extension rates corresponding to the initial onset of extensional flow enhanced crystallization ($\dot{\varepsilon}=0.01\ s^{-1}$), the point of maximum crystallinity ($\dot{\varepsilon}=0.05\ s^{-1}$), and the plateau observed in crystallinity ($\dot{\varepsilon}=0.5\ s^{-1}$) as measured by DSC. The samples were cut from around the axial midplane of the stretched filament and were mounted such that the extensional flow direction was aligned perpendicular to the beam direction and horizontally within the images in Fig. 7. The scattering pattern from the quiescent case which is not shown here is quite similar to the lowest extension rate shown in Fig. 7(a) as they both contain scattering ring patterns with azimuthal symmetry. These patterns are indicative of the randomly oriented and aligned finite lamellar stacks found within spherulites [Chu and Hsiao (2001)]. As the extension rate is increased, the azimuthal symmetry of the rings is broken with the appearance of bright peaks at the equator. These peaks are likely the result of preferential alignment of lamellar stacks in the flow direction and are strong evidence for the presence of a shish-kebab morphology [Keller and Kolnaar (1997); Samon *et al.* (1999)]. The intensity of these equatorial peaks, and thus the predominance of the shish-kebab morphology, is found to increase with increasing extension rate. However, it is interesting to note that over this same range in extension rate, from $0.05\ s^{-1}$ to $0.5\ s^{-1}$, the DSC measurements show a reduction in the degree of crystallinity.

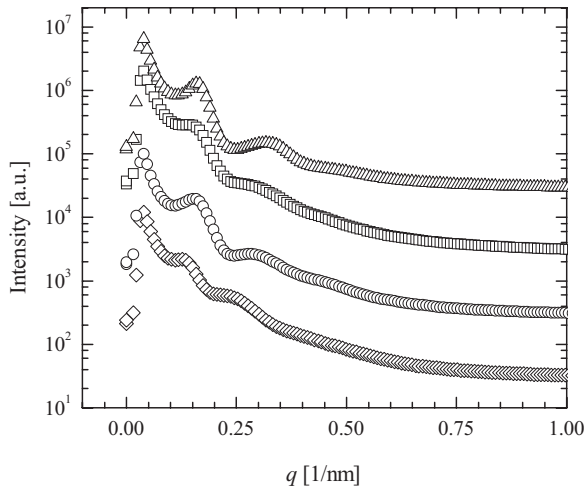

FIG. 8. Intensity of the scattering images presented in Fig. 7 as a function of scattering vector, q, for DP0401M. Included are results for the case of quiescent crystallization (◇) and crystallization following stretches of extension rates of $\dot{\varepsilon}=0.01\ s^{-1}$ (○), $\dot{\varepsilon}=0.05\ s^{-1}$ (□), and $\dot{\varepsilon}=0.5\ s^{-1}$ (△). All stretches were performed to an accumulated strain of $\varepsilon=5$.

In order to quantify the results from the SAXS measurements, the two-dimensional scattering data presented in Fig. 7 were circularly averaged and plotted as scattering intensity, I, in arbitrary units as a function of the wave vector, q. The resulting one-dimensional intensity profiles are presented in Fig. 8. For clarity, the scattering profiles are shifted vertically by multiplying the intensity values by an arbitrary constant to avoid overlap of the profiles. Strong peaks corresponding to the position of the rings observed in Fig. 7 are observed. In each case, the subsequent peaks are observed at locations corresponding to integer multiples of the primary peak. The crystals thus form a lamellar morphology independent of extension rate. The d-spacing or long period of the lamellar stacks is, however, found to be a function of extension rate. The long period of the unstretched case is approximately 52 nm. With increasing extension rate from 0.01 s^{-1} to 0.05 s^{-1} and finally to 0.5 s^{-1} the long period was found to decrease to $L_p=42$, 42, and 40 nm, respectively. It is interesting to note that the long period is not a strong function of the strength of the extensional flow only whether flow occurs at all. The SAXS data in Fig. 8 can also be used to determine the average thickness of the alternating crystalline and amorphous layers within each lamella. This is done by first extrapolating the SAXS data to large and small values of q and then using the methods described by Vonk and Kortleve [Vonk and Kortleve (1967)] and Strobl and Schneider [Strobl and Schneider (1980)] to calculate and analyze the resulting one-dimensional correlation function. The average thickness of the crystalline lamellae within the lamellar stacks was found remain essentially fixed largely independent of extension rate measuring $L_c=27$, 24, 26, and 24 nm for extension rates of 0.00, 0.01, 0.05, and 0.5 s^{-1}, respectively. Thus, it is clear from the SAXS measurements that the increased crystallinity in the stretched samples, as compared to the unstretched samples, is to some degree a result of the decrease in the thickness of the amorphous layer within the lamellar stacks induced by the alignment of polymer chains under extensional flow conditions.

In Fig. 9, the peak melting temperature calculated from the DSC measurements is plotted as a function of extension rate for both the DP0401M and the PB0200 samples. As seen in Fig. 9, the trends for both samples are qualitatively similar. The melting

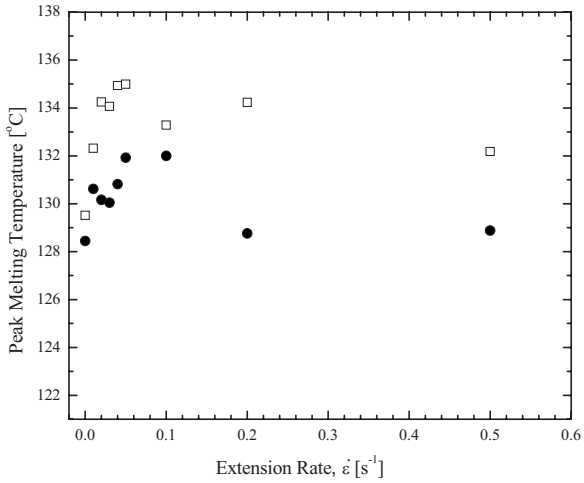

FIG. 9. Peak melting temperature as a function of extension rate for isotactic poly-1- butene samples at T_c=98 °C. Included are the solutions for DP0401M (□) at a fixed strain of ε=5.0 and PB 0200 (●) at a fixed strain of ε=4.0.

temperature of the stretched DP0401M sample increased from T_m=132 °C to 135 °C with increase in extension rate from $\dot{\varepsilon}$=0.01 s^{-1} to $\dot{\varepsilon}$=0.05 s^{-1}. This is a significant increase when compared to the unstretched sample which had a melting temperature of T_m =129 °C. The results are consistent with the trends in the percent crystallinity measurements shown in Fig. 5. According to Keller and Kolnaar (1997), polymer chain extension directly increases the melting temperature because it reduces the entropy and thus increases the free energy of an extended polymer chain when compared to a random coil. The increase in peak melting temperature with critical extension rate thus demonstrates the ability of extensional flows to increase the deformation of the polymer crystals and result in the formation of shish-kebab crystals in the final solid as seen by both microscopy and SAXS measurements. The trends in the peak melting temperature, and specifically, the decrease in peak melting temperature after a critical extension rate is consistent with the reduction in percent crystallinity seen in Fig. 5. However, as observed in the SAXS measurements in Fig. 7, this decrease is not coupled to a reduction in the amount of the shish-kebab morphology present in the final polymer. Beyond the critical extension rate the melt temperature for the DP0401M plateaus at around T_m=130 °C. This value is still larger than the quiescent case, but well below the maximum observed value. Additionally, although we do not present a plot showing the trends, these conclusions are further reinforced by the standard deviation of the melting temperature peaks which initially decreases with increasing extension indicating a more uniform final crystal size with increasing extension rate. However, as with all of these measurements, this trend is reversed for extension rates larger than the critical rate.

In order to quantify the effect of the accumulated strain on the crystallization under uniaxial extensional flow, a series of measurements was made at a fixed extension rate, but over a wide range of strains. In order to collect a sufficient amount of stretched polymer needed for DSC measurements, the experiments were limited to strains of $\varepsilon \leq 6.0$. The percent crystallinity as a function of Hencky strains is plotted in Fig. 10 at a fixed extension rate for the DP0401M sample at a fixed extension rates of $\dot{\varepsilon}$=0.05 s^{-1} and $\dot{\varepsilon}$=0.5 s^{-1}. The percent crystallinity is found to increase gradually with increasing strain; growing from 57% to 71% with increase in fixed Hencky strain for ε=2.0 to

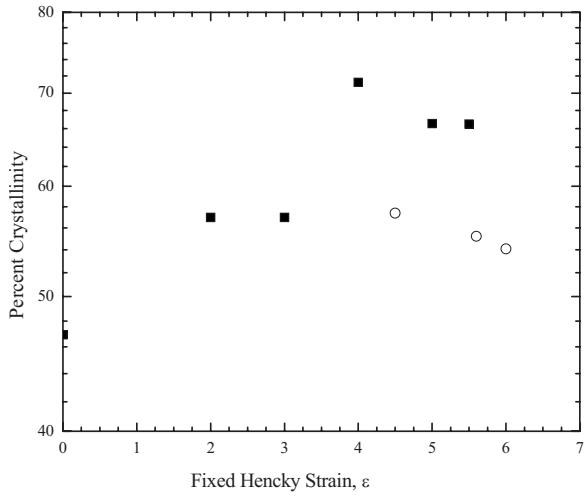

FIG. 10. Percent crystallinity as a function of series of strains for isotactic poly-1-butene samples. Included are the solutions for DP0401M at a fixed extension rate of $\dot{\varepsilon}=0.05\ s^{-1}$ (■) and $\dot{\varepsilon}=0.5\ s^{-1}$ (○).

$\varepsilon=4$ before appearing to level off within the uncertainty of these experiments. This increase in percent crystallinity with increase in strain demonstrates the sensitivity of extensional flows with respect to strains in enhancing the nucleation rate and crystallization kinetics. Above a strain of approximately $\varepsilon=4$, the percent crystallinity saturates as the extensional viscosity and polymer deformation reaches a steady-state under these flow conditions. Additionally, even at the fixed Hencky strain of $\varepsilon=2$, there is a significant increase in percent crystallinity compared to unstretched sample, which suggests that the nucleation density may have already increased drastically even under moderate strains.

D. Physical mechanism

Extensional flows are known to promote nucleation through the alignment and deformation of polymer chains. These highly oriented polymer chains crystallize more easily thereby increasing the nucleation rate compared to the quiescent state and result in shish-kebab rather than spherulite crystalline morphologies. The conventional wisdom is therefore that the crystals should nucleate and grow faster at higher extension rates due to the more rapid orientation and deformation of the chains. This is precisely what Hadinata *et al.* (2007) observed. They demonstrated that the onset time for crystallization of a high molecular weight poly-1-butene decreases with increasing extension rate. However, as shown in Fig. 5, although the filaments might crystallize more quickly with increasing extension rate, we observed a maximum in the percent crystallinity at the extension rate of $\dot{\varepsilon}=0.1\ s^{-1}$ and $\dot{\varepsilon}=0.05\ s^{-1}$ for PB0200 and DP0401M samples, respectively. A similar maximum was not observed with rate in melt spinning experiments of poly-1-butene by Samon *et al.* (2000), although the range of take up rates studied was rather limited.

There are a number of possible explanations for the presence of the maximum in the data. First, we note that the time scales of these experiments are found to be close to crystallization onset times observed in Hadinata *et al.* (2007). This observation suggests that the extensional flow might be deforming the nucleated and nucleating crystals and violating the Janeschitz-Kriegel protocol. For instance, at the Hencky strain of $\varepsilon=4$, using a polymer very similar to our PB0200, Hadinata *et al.* (2007) found crystallization

onset time for the extension rate of $\dot{\varepsilon}=0.1\ \ s^{-1}$ is approximately 30 s. In our experiments, for PB0200 the duration of the experiment for the same strain and extension rate is approximately about 20 s. We, however, feel that this mechanism is unlikely the cause of the observed maximum because unlike Hadinata *et al.* (2007), a sharp increase in the extensional viscosity, indicative of crystallization during the stretch, was not observed in any of our experiments. Additionally, we did not observe a maximum in crystallinity with strain or equivalently the duration of the experiment.

The observed maximum crystallinity might also be due to the high polydispersity of the samples. The initial conformation and molecular weight of the chains nucleating to form the shish-kebabs will change with extension rate; increasing extension rate will increasingly orient smaller tube and chain segments in the flow direction. However, if we were indeed crystallizing more of the lower molecular weight polymers in the melt, one might expect the degree of crystallinity to go up not down with increasing rate. The results for the two different average molecular weight samples clearly demonstrate that the lower molecular weight sample is more crystalline under both quiescent and flow-induced conditions. Although polydispersity does not appear to be the root cause of the maximum in the data, the effect of molecular weight cannot be discounted until measurement of extensional flow-induced crystallization are performed on monodisperse samples. It is our intention to perform these measurements in the near future. Another possibility is that increasing extension rate promotes the inclusion of entanglement points and defects in the nucleation sites, although this hypothesis is difficult to test. Yet another hypothesis that was considered was that the maximum in the degree of crystallinity was the result of viscous heating effects. However, the Brinkman number in all cases was small enough, $Br<10^{-3}$, that viscous heating effects should be negligible [Bird *et al.* (1987)].

The maximum and subsequent plateau of the crystallinity with increasing extension rate could also be the result of the finite time it takes nucleation to occur. As the extension rate increases, the polymers tubes and chains are aligned and oriented. The increased extension rate also increases the probability that two polymer chains or segments of the same chain will collide with one another with the potential to nucleate a crystal. In fact, the collision rate has been shown to increase with the root-mean-square projection of the chain dimension in the deformation direction, which is in turn proportional to the imposed extension rate [Tripathi *et al.* (2006)]. However, at the same time increasing the extension rate also reduces the time duration that two colliding chains have to crystallize before the extensional flow moves the two chains apart. It is possible that at the critical extension rate, the time scale of the flow becomes faster than the time scale for crystallization resulting in the observed maximum in the degree of crystallization. The plateau could be the result of nucleation of crystals not during the flow, but just subsequent to the flow while the tubes and chains are still aligned and are beginning to relax back to their equilibrium state.

The maximum observed in the percent crystallinity might also stems from the effectiveness with which extensional flows increase the nucleation density and subsequent rate of crystallization of polymer melts. The increased crystallization rate, which was directly observed by Hadinata *et al.* (2007), could result in an increase in crystalline defects that would reduce the overall percent crystallinity. One thing is clear, to fully understand this maximum in percent crystallization with increasing extension rate, future studies will likely be require the investigation of a number of different polymer melts and a detailed study of the crystallization kinetics with *in situ* SAXS measurements.

IV. CONCLUSIONS

The extensional flow-induced crystallization of two commercial grade poly-1-butene DP0401M and PB0200 samples were investigated using filament stretching rheometer as a function of extension rate and accumulated Hencky strains. All the rheology measurements are performed at a reference temperature of $T_c = 98\,^{\circ}\mathrm{C}$ using the Janeschitz-Kriegl protocol. The shear rheology of the PB0200 samples demonstrated a higher relaxation time and higher complex viscosity compared to low molecular weight DP0401M sample.

A series of transient extensional rheology measurements was performed on both the DP0401M and the PB0200 samples using a filament stretching extensional rheometer coupled with an oven. The extensional rheology of both the samples is insensitive to all the tested strain rates showing only minimal strain hardening. However, even in the absence of significant extensional thickening the alignment of the tube of entanglements within the filament under extensional flow was sufficient to dramatically affect the crystallization dynamics of both polymers.

To quantify the percent crystallinity achieved in the stretched polymers, a series of DSC and SAXS measurements was performed on the samples of DP0401M and PB0200 stretched over a broad range of extension rates and accumulated Hencky strains. The degree of crystallinity was found to increase by as much as 50% when compared to the unstretched sample. The increase in percent crystallinity was shown to be due to the effective orientation of tube of confinements around the polymer chains, which increases with extension rate, thereby enhancing the formation of the thread-like precursors, which are responsible for the formation of the crystals in the shish-kebab morphology. The increase in crystallinity was not a monotonic function of extension rate for either sample although it was found to be monotonic with accumulated strain. In each case, there is a critical extension rate above which a decrease in the crystallinity is observed with increasing extension rate before reaching a plateau at high rates. This observation indicates that there is an optimal extension rate for achieving the maximum degree of crystallinity in these samples. The generality of this observation for different polymers and different polymer architectures is still to be investigated.

ACKNOWLEDGMENTS

The authors would like to thank the National Science Foundation for the generous support of this research under Grant No. CBET-0651888 and the UMASS MRSEC for the use of their DSC and shear rheology facilities. The use of the National Synchrotron Light Source at Brookhaven National Laboratory was supported by the U.S. Department of Energy under Contract No. DE-AC02-98CH10886. Finally, the authors would like to thank Vikram K. Daga for his help with SAXS measurements.

References

Acierno, S., N. Grizzuti, B. Palomba, and H. H. Winter, "Effect of molecular weight on the flow-induced crystallization of isotactic poly(1-butene)," Rheol. Acta **42**, 243–250 (2003).

Alfonso, G. C., F. Azzurri, and M. Castellano, "Analysis of calorimetric curves detected during the polymorphic transformation of isotactic polybutene-1," J. Therm. Anal. Calorim. **66**, 197–207 (2001).

Anna, S. L., and G. H. McKinley, "Elasto-capillary thinning and breakup of model elastic liquids," J. Rheol. **45**, 115–138 (2001).

Anna, S. L., G. H. McKinley, D. A. Nguyen, T. Sridhar, S. J. Muller, J. Huang, and D. F. James,

"An inter-laboratory comparison of measurements from filament stretching rheometers using common test fluids," J. Rheol. **45**, 83–114 (2001).

Azzurri, F., A. Flores, G. C. Alfonso, I. Sics, B. S. Hsiao, and F. J. B. Calleja, "Polymorphism of isotactic polybutene-1 as revealed by microindentation hardness. Part II: Correlations to microstructure," Polymer **44**, 1641–1645 (2003).

Bhattacharjee, P. K., J. Oberhauser, G. H. McKinley, L. G. Leal, and T. Sridhar, "Extensional rheometry of entangled solutions," Macromolecules **35**, 10131–10148 (2002).

Bird, R. B., R. C. Armstrong, and O. Hassager, *Dynamics of Polymeric Liquids: Vol. 1 Fluid Mechanics* (Wiley, New York, 1987).

Chai, C. H., Q. Auzoux, H. Radrianatandro, P. Navard, and J. M. Haudin, "Influence of pre-shearing on the crystallization of conventional and metallocene poly-ethylenes," Polymer **44**, 773–782 (2003).

Chu, B., and B. S. Hsiao, "Small-angle x-ray scattering of polymers," Chem. Rev. **101**, 1727–1762 (2001).

Eder, G., and H. Janeschitz-Kriegel, in *Processing of Polymers*, edited by H. E. H. Meijer (Wiley-VCH, New York, 1997).

Elmoumni, A., and H. H. Winter, "Large strain requirements for shear induced crystallization of isotactic polypropylene," Rheol. Acta **45**, 793–801 (2006).

Elmoumni, A., H. H. Winter, A. Waddon, and H. Fruitwala, "Correlation of material and processing time scales with structure development in isotactic polypropylene crystallization," Macromolecules **36**, 6453–6461 (2003).

Haas, T. W., and B. Maxwell, "Effects of shear stress on crystallization of linear polyethylene and polybutene-1," Polym. Eng. Sci. **9**, 225–241 (1969).

Hadinata, C., D. Boos, C. Gabriel, E. Wassner, M. Rullmann, N. Kao, and M. Laun, "Elongation-induced crystallization of a high molecular weight isotactic polybutene-1 melt compared to shear-induced crystallization," J. Rheol. **51**, 195–215 (2007).

Hoffman, J. D., and J. I. Laurritzen, "Crystallization of bulk polymers with chain folding: Theory of growth of lamellar spherulites," J. Res. Natl. Bur. Stand., Sect. A **65A**, 297–336 (1961).

Janeschitz-Kriegl, H., "How to understand nucleation in crystallizing polymer melts under real processing conditions," Colloid Polym. Sci. **281**, 1157–1171 (2003).

Janeschitz-Kriegl, H., and G. Eder, "Basic concepts of structure formation during processing of thermoplastic materials," J. Macromol. Sci., Chem. **A27**, 1733–1756 (1990).

Janeschitz-Kriegl, H., G. Eder, M. Stadlbauer, and E. Ratajski, "A thermodynamic frame for the kinetics of polymer crystallization under processing conditions," Monatsch. Chem. **136**, 1119–1137 (2005).

Janeschitz-Kriegl, H., E. Ratajski, and M. Stadlbauer, "Flow as an effective promotor of nucleation in polymer melts: A quantitative evaluation," Rheol. Acta **42**, 355–364 (2003).

Keller, A., and H. W. H. Kolnaar, in *Processing of Polymers*, edited by H. E. H. Meijer (Wiley-VCH, New York, 1997).

Kumaraswamy, G., J. A. Kornfield, F. Yeh, and B. S. Hsiao, "Shear-enhanced crystallization in isotactic polypropylene 3. Evidence for a kinetic pathway to nucleation," Macromolecules **35**, 1762–1769 (2002).

Li, L. B., and W. H. de Jeu, "Shear-induced smectic ordering as a precursor of crystallization in isotactic polypropylene," Macromolecules **36**, 4862–4867 (2003).

Liedauer, S., G. Eder, H. Janeschitz-Kriegl, P. Jerschow, W. Geymayer, and E. Ingolic, "On the kinetics of shear-induced crystallization in polypropylene," Int. Polym. Process. **8**, 236–244 (1993).

McHugh, A. J., J. Lyngaae-Jsrgensen, and K. Sondergaard, "Rheo-physics of multiphase polymeric system," TECHNOMIC Publishing No. 227 (1995).

McKinley, G. H., and T. Sridhar, "Filament-stretching rheometry of complex fluids," Annu. Rev. Fluid Mech. **34**, 375–415 (2002).

Pennings, A. J., and A. M. Kiel, "Fractionation of polymers by crystallization from solution. 3. On morphology of fibrillar polyethylene crystals grown in solution," Kolloid Z. Z. Polym. **205**, 160 (1965).

Pennings, A. J., J. M. Vanderma, and H. C. Booij, "Hydrodynamically induced crystallization of polymers from solution. 2. Effect of secondary flow," Kolloid Z. Z. Polym. **236**, 99–111 (1970).

Pogodina, N. V., S. K. Siddiquee, J. W. van Egmond, and H. H. Winter, "Correlation of rheology and light scattering in isotactic polypropylene during early stages of crystallization," Macromolecules **32**, 1167–1174

(1999).

Rothstein, J. P., and G. H. McKinley, "A comparison of the stress and birefringence growth of dilute, semi-dilute and concentrated polymer solutions in uniaxial extensional flows," J. Non-Newtonian Fluid Mech. **108**, 275–290 (2002).

Samon, J. M., J. M. Schultz, B. S. Hsiao, S. Seifert, N. Stribeck, I. Gurke, G. Collins, and C. Saw, "Structure development during the melt spinning of polyethylene and poly(vinylidene fluoride) fibers by in situ synchrotron small- and wide-angle x-ray scattering techniques," Macromolecules **32**, 8121–8132 (1999).

Samon, J. M., J. M. Schultz, B. S. Hsiao, J. Wu, and S. Khot, "Structure development during the melt spinning and subsequent annealing of polybutene-1 fibers," J. Polym. Sci., B, Polym. Phys. **38**, 1872–1882 (2000).

Seki, M., D. W. Thurman, J. P. Oberhauser, and J. A. Kornfield, "Shear-mediated crystallization of isotactic polypropylene: The role of long chain-long chain overlap," Macromolecules **35**, 2583–2594 (2002).

Sentmanat, M., O. Delgadillo-Velázquez, and S. G. Hatzikiriakos, "Crystallization of an ethylene-based butene plastomer: The effect of uniaxial extension," Rheol. Acta **49**, 931–939 (2010).

Somani, R. H., L. Yang, B. S. Hsiao, T. Sun, N. V. Pogodina, and A. Lustiger, "Shear-induced molecular orientation and crystallization in isotactic polypropylene: Effects of the deformation rate and strain," Macromolecules **38**, 1244–1255 (2005).

Stadlbauer, M., H. Janeschitz-Kriegl, G. Eder, and E. Ratajski, "New extensional rheometer for creep flow at high tensile stress. Part II. Flow induced nucleation for the crystallization of ipp," J. Rheol. **48**, 631–639 (2004a).

Stadlbauer, M., H. Janeschitz-Kriegl, M. Lipp, G. Eder, and R. Forstner, "Extensional rheometer for creep flow at high tensile stress. Part I. Description and validation," J. Rheol. **48**, 611–629 (2004b).

Strobl, G. R., and M. Schneider, "Direct evaluation of the electron density correlation function of partially crystalline polymers," J. Poly. Sci. **18**, 1343–1359 (1980).

Swartjes, F. H. M., G. W. M. Peters, S. Rastogi, and H. E. H. Meijer, "Stress induced crystallization in elongational flow," Int. Polym. Process. **18**, 53–66 (2003).

Tirtaatmadja, V., and T. Sridhar, "A filament stretching device for measurement of extensional viscosity," J. Rheol. **37**, 1081–1102 (1993).

Tripathi, A., G. H. McKinley, K. C. Tam, and R. D. Jenkins, "Rheology and dynamics of associative polymers in shear and extension: Theory and experiments," Macromolecules **39**, 1981–1999 (2006).

van Meerveld, J., G. W. M. Peters, and M. Hütter, "Towards a rheological classification of flow induced crystallization experiments of polymer melts," Rheol. Acta **44**, 119–134 (2004).

Vleeshouwers, S., and H. E. H. Meijer, "A rheological study of shear induced crystallization," Rheol. Acta **35**, 391–399 (1996).

Vonk, C. G., and G. Kortleve, "X-ray small angle scattering of bulk polyethylene II. Analysis of the scattering curve," Kolloid Z. Z. Polym. **220**, 19–24 (1967).

Winter, D., C. D. Eisenbach, J. A. Pople, and A. P. Gast, "Small-angle x-ray scattering studies of poly(arylethinylene): Molecular conformation in solution and orientational ordering in rod-coil ionomer blends," Macromolecules **34**, 5943–5949 (2001).